LANGMUIR

pubs.acs.org/Langmuir Article

Magnesium-Induced Rapid Nucleation of Tetrahydrofuran Hydrates

Karey Maynor, Awan Bhati, Mark Hamalian, Ana Maria Ferraria, Ana Paula da Costa Ribeiro, Ana S. Moita, and Vaibhav Bahadur*

Cite This: https://doi.org/10.1021/acs.langmuir.4c02882 Read Online

ACCESS | Metrics & More | Article Recommendations | Supporting Information

ABSTRACT: Hydrates are ice-like crystalline structures of hydrogen-bonded water molecules that trap a guest molecule. Hydrates have several applications, including carbon sequestration, gas separation, desalination, etc. A classical major challenge associated with artificial hydrate formation is the very long induction time to nucleate hydrates. This has spurred the development of multiple chemical, mechanical, and electrical strategies to promote nucleation. Presently, we discover that magnesium can significantly promote the nucleation of tetrahydrofuran (THF) hydrates. While magnesium has been recently shown (by our group) to promote the formation of carbon dioxide hydrates (gas−liquid system), this study discovers that the benefits of magnesium extend to liquid−liquid hydrate systems as well. Experiments show that magnesium reduces the induction time for THF hydrate nucleation with deionized (DI) water and saltwater by six and eight times, respectively. Magnesium-induced nucleation rate enhancements for hydrate formation with DI water and saltwater were 12 and 99 times, respectively. Importantly, we demonstrate near-instantaneous nucleation when magnesium is introduced after the hydrate-forming system reaches suitable thermodynamic conditions. We conduct statistically significant measurements of nucleation and XPS analysis to identify the underlying mechanisms responsible for nucleation. We discuss multiple phenomena at play, including chemical and mechanistic promotion pathways. The formation of hydrogen bubbles and the presence of magnesium ions in solution are seen as important to magnesium-based nucleation promotion. Importantly, very low amounts of Mg are consumed in this process unlike in traditional chemical promotion techniques. Overall, our discovery can enable on-demand nucleation of liquid−liquid hydrate systems, which is critical to the development of several applications.

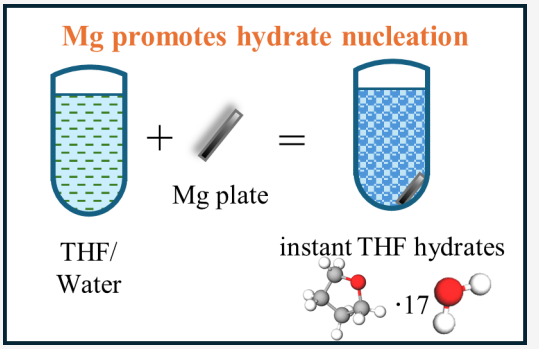

INTRODUCTION

Clathrate hydrates are crystalline structures formed by hydrogen-bonded water molecules that trap a guest molecule in a lattice cage. Guest molecules can include gases such as methane (CH_4) and carbon dioxide (CO_2) or liquids such as tetrahydrofuran (THF). The size of the guest molecule and its interactions with water determine the type of hydrate formed. Each hydrate type has a different volume and shape cavity.[1] Small molecules such as CH_4 or CO_2 form cubic sI hydrates, larger molecules such as tetrahydrofuran (THF) form cubic sII hydrates, and even larger molecules form hexagonal sH hydrates.[2] Clathrate hydrates have gained interest for many uses such as carbon dioxide (CO_2) sequestration,[3−5] desalination,[6] gas separation,[7] gas storage,[8,9] and as an energy carrier.[10]

This study focuses on the nucleation of THF hydrates; THF (C_4H_8O) forms sII hydrates with water at a 1:17 stoichiometric ratio—$C_4H_8O{\cdot}17H_2O$. THF hydrates are of particular interest as previous studies have shown that findings/insights from studies on THF hydrate formation can be applied to CH_4 and CO_2 hydrate formation.[11,12] Studying THF hydrates is easier than studying gas hydrates since THF hydrates form at atmospheric pressures and temperatures below 4.4 °C.[13,14] In contrast, clathrate hydrates of CO_2 and CH_4 require high pressures, which significantly increase the complexity of experiments and hinder measurements due to the requirements of a pressure cell for conducting such experiments. Furthermore, CH_4 and CO_2 hydrate formation generally involves two-phase systems (liquid water and gas guest molecules), which adds another layer of complexity in the heat and mass transfer analysis. On the other hand, THF and water are miscible fluids, so THF hydrate systems are single-phase and can be assumed to be homogeneous.[15] For these reasons, THF hydrates are widely used as a surrogate for more complex hydrate systems.[16,17] THF hydrates have been used to quantify the performance of thermodynamic and kinetic promoters such as salts,[18] mechanical agitation,[19] electronucleation,[20,21] and other technologies to promote hydrate formation.[22]

Received: July 26, 2024
Revised: September 21, 2024
Accepted: September 23, 2024

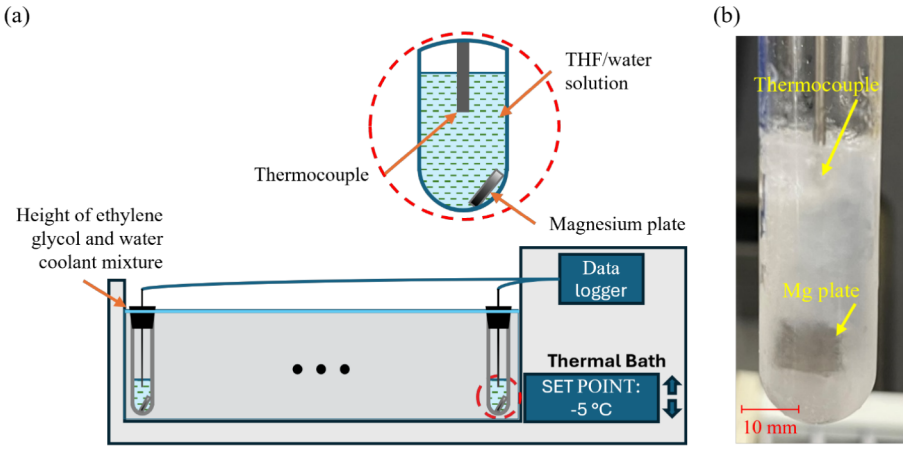

Figure 1. (a) Schematic depiction of the experimental setup. (b) THF hydrate with magnesium plate in the test tube.

Furthermore, it has been shown that the use of THF in binary hydrate systems increases the gas uptake of both hydrogen and carbon dioxide.[9,23,24] Other applications of THF hydrates include usage as a thermodynamic promoter.[25] The addition of THF significantly lowers the formation pressure of hydrogen hydrates to industrially achievable ranges[9,23] (from 300 MPa with no THF to 5 MPa with THF); this opens up promising avenues to enable new concepts for the storage and transport of hydrogen. THF hydrates also promote the formation of other gas hydrates, such as CO_2 and CH_4.

Significant classical challenges associated with artificial hydrate formation include the long induction (wait) times for nucleation and slow growth rates. Hydrate nucleation can take hours to days even under favorable thermodynamic conditions, unless nucleation promotion techniques are employed. All types of hydrate systems (liquid−liquid and liquid−gas) are associated with significant induction time (delay in nucleation). Sluggish formation is a dealbreaker for most energy-relevant applications, which require hydrate formation at rapid rates.

Multiple studies have reported induction times, formation times, and nucleation percentages (percentage of samples that nucleated hydrates) for THF hydrates.[10,12,20,26−28] A previous study by the present group found that the nucleation percentage for THF hydrates was less than 10% in 180 min in the absence of promoters at −5 °C (significant subcooling of 9.4 °C).[20] Application of an electric field (electronucleation) led to 100% nucleation with induction times as low as 6 s. Another study reported that over 85% of THF samples nucleated at the same temperature of −5 °C with an average induction time of 156.5 min.[26] Both these studies highlight the long induction times and stochastic nature of nucleation, which has been confirmed by many other studies.[10,26] THF hydrates do form more consistently with higher subcooling;[12,26] however, increased subcooling is associated with increased energy consumption, which is undesirable for applications. Liu et al.[12] formed THF hydrates in porous media, showing that smaller cavities and a higher degree of subcooling promoted nucleation with average induction times ranging from 40 to 300+ minutes. This study also showed evidence of a memory effect with a 54% average reduction in the induction time when hydrate-dissociated water was used in subsequent experiments. However, other studies have not shown evidence of a memory effect for THF hydrates[11]—if a memory effect does in fact exist, it appears to be reactor- and condition-specific. Nanoparticles have been shown to promote THF hydrate formation.[27,28] Sun et al. found that SiO_2 nanoparticles reduced the induction time from 45 min with no promoter to less than 30 min.

This study reports the discovery of the nucleation-promoting benefits of magnesium for THF hydrates. This work is inspired by a recent study[29] from the same group which discovered that magnesium can enhance the nucleation rate of CO_2 hydrates by 3000X in a quiescent environment. At present, we study the nucleation promotion benefits of magnesium for THF hydrates, which is a two-miscible liquids-based system in contrast to the gas−liquid system of CO_2 hydrates. Both these systems are very distinct from a mass and heat transfer perspective. Extensive experimentation is conducted to quantify magnesium-induced reduction in induction time with deionized (DI) water and saltwater. Multiple parameters are varied to quantify their influence on hydrate formation. Several experiments are conducted to obtain insights into the mechanisms underlying nucleation promotion along with postexperiments characterization of magnesium surfaces via XPS studies.

EXPERIMENTAL SECTION

Experimental Setup and Procedure. A schematic depicting the experimental setup used in this study is shown in Figure 1. This setup and experimentation protocol was modified from our previous work on THF hydrates.[20] For statistically meaningful results, nucleation measurements were conducted with 15 THF−water mixtures in separate test tubes in a single run. The test tubes were closed (to prevent evaporation of THF) with a rubber stopper, which also held a Type-T thermocouple (accuracy is ±1 °C) which was fully immersed in the THF−water solution. A 15 L temperature-controlled bath filled with a 50/50 mix of water and ethylene glycol was used to provide isothermal temperatures. All test tubes were fully submerged in a cooling bath.

THF (≥99.9%) and deionized (DI) water (conductivity of ≤1.0 μMHOS) in a 1:15 molar ratio were freshly mixed before each experimental run, and each test tube was filled with 5 mL of the solution. A ratio of 1:15 was chosen since the stoichiometric molar ratio for THF hydrate formation is 1:17, and the aim was to preferentially form THF hydrates over ice. The tubes were loaded into a rack and submerged into a cooling bath set at 5 °C. The tubes equilibrated for 15 min at 5 °C before the bath set point was adjusted to −5 °C, thereby providing a temperature subcooling of 9.4 °C (hydrate formation temperature is 4.4 °C). Each experiment ran until all the samples nucleated or for 18 h (maximum duration of experiments). For experiments involving magnesium, a 0.2 g piece of

https://doi.org/10.1021/acs.langmuir.4c02882
Langmuir XXXX, XXX, XXX−XXX

Table 1. Description of Conditions in Various Experiments in This Study

Exp. ID	Description of experiment	Mg used	Water	THF:water ratio	Cooling conditions
1	Control experiment	No	Deionized	1:15	Initial temperature: 5 °C Subcooling: 9.4 °C
2	Influence of Mg (Video 1)	Yes	Deionized	1:15	Initial temperature: 5 °C Subcooling: 9.4 °C
3	Influence of Mg and accelerated cooling	Yes	Deionized	1:15	Initial temperature: −5 °C Subcooling: 9.4 °C
4	Instantaneous nucleation (Video 2)	Yes	Deionized	1:15	Initial temperature: −5 °C Subcooling: 9.4 °C
5	Influence of 3-phase line	Yes	Deionized	1:15	Initial temperature: 5 °C Subcooling: 9.4 °C
6	Control experiment with saltwater	No	Saltwater	1:15	Initial temperature: 5 °C Subcooling: 7.6 °C
7	Influence of Mg with saltwater	Yes	Saltwater	1:15	Initial temperature: 5 °C Subcooling: 7.6 °C

magnesium alloy (AZ31) was added to each test tube prior to the tubes being submerged in the bath. Each piece of magnesium alloy was 1 mm thick and 10 mm × 10 mm square. The choice of this alloy was based on our previous study[29] which discovered the benefits of magnesium for nucleating CO_2 hydrates.

Several variations of the experimental procedure described above were run to analyze the factors influencing induction times. The first variation investigated whether the cooling process had an impact on the induction time and nucleation rate. Accordingly, the cooling bath was set to −5 °C before the tubes were submerged; therefore, they experienced a stronger thermal shock and accelerated cooling from ambient temperature to −5 °C. The second variation was conducted to determine if near-instantaneous nucleation was possible. For these experiments, the standard cooling process was used to equilibrate the tubes to −5 °C, at which point a magnesium plate was dropped into the solution to see if the sudden introduction of magnesium affected the induction time differently than in other experiments.

Separately, experiments were also conducted to study the influence of the presence of a three-phase contact line (solution−air with THF vapor-Mg) on the nucleation. This is related to the present group's discovery that the three-phase line promotes nucleation of ice.[30] Experiments were also conducted with saltwater, noting that hydrate formation is challenging with salt water.[31,32] A 3.5 wt % NaCl concentration in DI water was used to mimic oceanwater concentration. Table 1 summarizes the conditions associated with various experiments in the present study.

Detecting Nucleation. Nucleation was detected by a spike in the temperature of the hydrate-forming solution (Figure 2). This is a commonly used method for determining ice nucleation and has also been used for previous studies on hydrates.[19,20] At the onset of nucleation, heat associated with crystallization is released suddenly. The equilibrium temperature associated with THF hydrate formation in DI water is 4.4 °C. Based on the distance of the thermocouple tip to the actual point of nucleation (not being controlled), this temperature spike was observed to be above 0 °C and below 4 °C; this confirms the absence of ice. It is noted that the equilibrium temperature for THF hydrate formation from saltwater is lower than that associated with forming hydrates from pure water; according to the literature,[26,33,34] the equilibrium temperature is approximately 1.5 °C lower. However, we conducted a measurement and found that the equilibrium temperature for THF hydrate formation with saltwater is 2.6 °C (1.8 °C lower).

As a second check to confirm the absence of ice, the hydrates formed in each experimental run were held overnight at a temperature below the equilibrium temperature of the THF hydrates (4.4 °C) but above the melting point of ice. For non-saltwater tests, this temperature was 2 °C, and for saltwater tests, this temperature was 0 °C due to the freezing point depression caused by the presence of salts. The overnight stability (lack of dissociation) of the formed hydrates confirms the absence of ice formation.

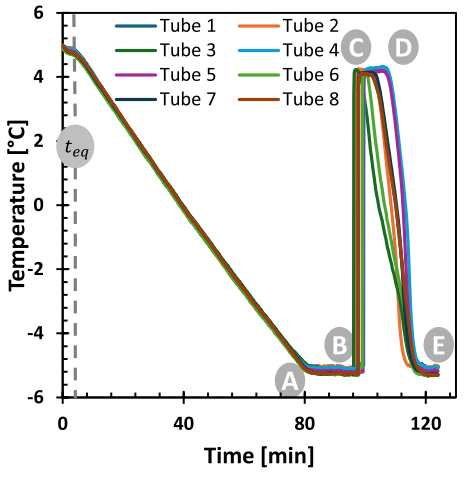

Figure 2. Temperature−time plot showing instantaneous nucleation of THF hydrates upon the introduction of magnesium. A−B: samples equilibrated at −5 °C for 15 min. B−C: at point B, a Mg plate was dropped into each test tube resulting in near-instantaneous nucleation. From B to C, hydrate formation releases heat and the temperature spikes to near-equilibrium temperature for THF hydrates. C−D: hydrate formation propagates through the entire volume of solution. D−E: hydrate plug cools down to the bath temperature of −5 °C.

RESULTS AND DISCUSSION

Experiments to Study Nucleation of THF Hydrates. Video 1 and Figure S1 illustrate a "typical" experiment wherein magnesium promotes nucleation of THF hydrates. The main parameter used in our work to study nucleation is the induction time. Induction time is defined as the time interval between when a sample nucleated and when it reached hydrate formation equilibrium temperature.[1] Our study finds that magnesium promotes THF hydrate nucleation and dramatically reduces the induction time. This is best illustrated by the "instantaneous" nucleation experiments, the results of which are outlined in Table 2. Temperature variation throughout the experimental run is depicted in Figure 2. Each tube was prepared as specified previously without the magnesium plate and then cooled to −5 °C (point A in Figure 2). The system was left to equilibrate for 15 min at −5 °C (A−B) to allow for any nonpromoted hydrate nucleation without the presence of Mg. Two out of the 10 tubes were found to nucleate in this duration (can be attributed to stochasticity of nucleation). After this waiting period, a piece of Mg was dropped into each of the remaining tubes (point B) in series. Near-instantaneous nucleation (depicted in video 2) was observed in all the remaining tubes (B−C) as indicated by the temperature spike to the hydrate nucleation temperature of 4.4 °C.

To ensure that mechanical agitation was not responsible for this nucleation, a separate experiment was conducted, wherein multiple test tubes were shaken vigorously for 30 s after they were cooled to −5 °C. No nucleation was observed in this case, highlighting the role of magnesium in nucleation promotion. All test tubes were observed to hold their temperature at 4.4 °C, indicating further hydrate growth

https://doi.org/10.1021/acs.langmuir.4c02882
Langmuir XXXX, XXX, XXX−XXX

Table 2. Summary of Induction Time Data for Various Experiments in This Study

Exp. ID	Test type	Mean induction time (min)	Standard deviation (min)	Minimum induction time (min)	Maximum induction time (min)	Tubes nucleated (%)
1	DI water without Mg promotion	376	141	258	685	60
2	DI water with Mg promotion	62.2	12.6	34.5	98.5	100
3	DI water with Mg and accelerated cooling	17.9	11	0.4	46.6	100
5	DI water with Mg and 3-phase line	55.2	12.3	33.1	79.8	100
6	Salt water without Mg promotion	471	315	182	909	14
7	Salt water with Mg promoter	56	9.5	28.6	72.9	100

(C−D), with the hydrate formation front advancing in all directions. The width of the spike (C−D) indicates the duration for apparent full conversion to hydrates. Subsequently, the temperature was observed to drop back to −5 °C (D−E), equilibrating with the cooling bath.

Next, the results of experiments to quantify induction time using the procedure described in the previous section (equilibration at 5 °C followed by cooling to −5 °C) are presented (these do not include the near-instantaneous nucleation results described in Figure 2). It is seen that the presence of the Mg plate significantly improved the induction time and nucleation percentage (Figure 3) significantly. The

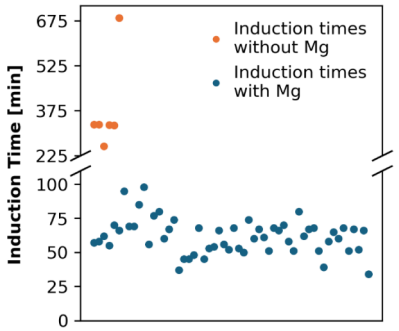

Figure 3. Induction time associated with THF hydrate formation in DI water with and without magnesium promotion. Six data points are shown for cases in which nucleation occurred without magnesium, also noting that nucleation occurred in only 60% of such solutions. 56 data points are shown with magnesium present, which resulted in 100% nucleation.

average induction time was 376 min in the absence of the Mg plate, whereas the average induction time in the presence of the Mg plate was 62 min. This represents a 6X decrease in the induction time. Moreover, the percentage of samples that nucleated without Mg was 60% (this includes the two tubes from the results in Figure 2 that nucleated before the introduction of Mg). In contrast, 100% of samples nucleated in the presence of the Mg plate. Figure 3 illustrates the significant impact of magnesium on reducing the induction time, particularly with DI water.

Similar results were observed for the experiments conducted with saltwater. The average induction time for hydrate nucleation from saltwater without Mg was 471 min; this underscores the inhibiting influence of salt ions on hydrate nucleation. Significantly, Mg reduced this induction time to 56 min, which is an 8.4 times reduction. The percentage of saltwater samples that nucleated without Mg was 14%, while 100% samples nucleated in the presence of Mg.

Table 2 presents a summary of the detailed induction time data (minimum, maximum, average, and standard deviation) for all experiments.

The influence of the cooling rate on hydrate nucleation was also studied. Figure 4 shows all eight experiments for hydrate

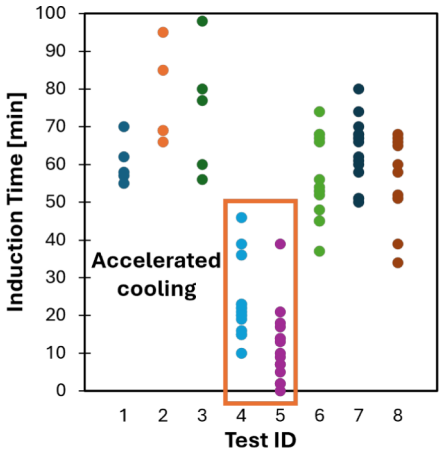

Figure 4. Compilation of the induction time distribution for all hydrate formation experiments using DI water.

formation in the presence of magnesium (experiments 2 and 3 as outlined in Table 1). Tests 4 and 5 correspond to experiments with accelerated cooling; results indicate that accelerated cooling reduced the induction time compared to the slower cooling experiments. These experiments deviated from the standard procedure in that the cooling bath was precooled to −5 °C, so the ramp down time was much shorter. When the samples experienced the initial colder bath temperature, the average induction time reduced from 62 to 17.9 min—a further 3.5 times reduction. This result can be attributed to a stronger driving force for nucleation provided by the faster cooling rate.

Two additional experiments were conducted to further investigate specific aspects of the influence of magnesium on the THF hydrate nucleation. First, the influence of the 3-phase (THF−water solution−air with THF vapor-Mg) contact line on nucleation was characterized. In our past study, the 3-phase line has been identified as the point of nucleation.[29,30] For these experiments, a longer piece of magnesium plate was used such that a portion of the plate protruded above the THF−water solution in the glass tube. This creates a contact line between the solid plate, the THF/water liquid, and the THF/water vapor and air. Figure 5 shows a comparison of the temperature profiles for a magnesium-promoted experiment with the plate fully submerged versus partially submerged (3-phase line). As seen in Figure 5, the partially submerged plates result in larger and cleaner temperature spikes. The jagged and

https://doi.org/10.1021/acs.langmuir.4c02882
Langmuir XXXX, XXX, XXX−XXX

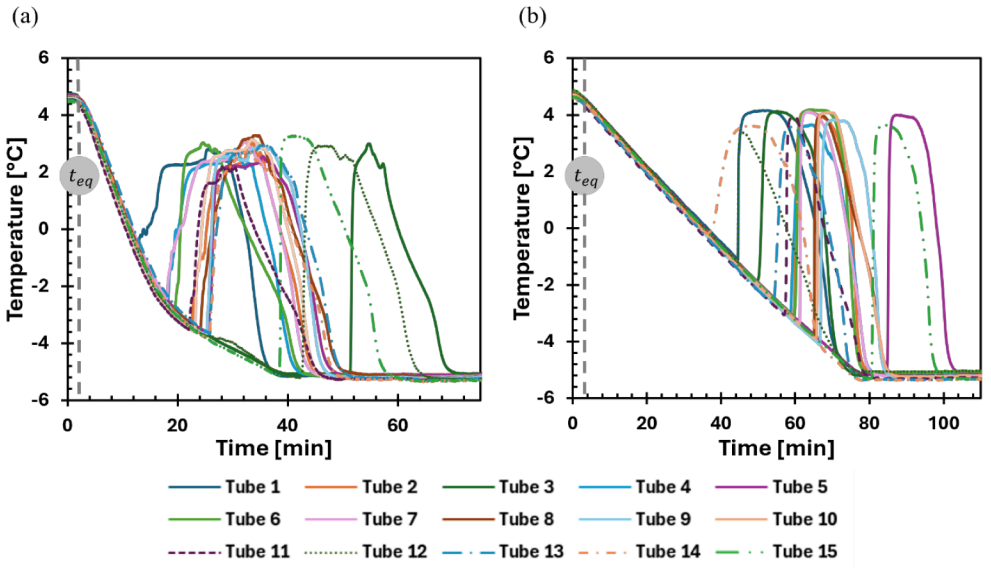

Figure 5. (a) Temperature profiles associated with hydrate formation with magnesium plates fully submerged in solution. (b) Temperature profiles associated with hydrate formation with magnesium plates partially submerged (3-phase contact line exists).

irregular nature of the temperature profiles in some of the submerged plate experiments indicates that multiple secondary nucleation events are occurring. However, a comparison of induction times (Table 2) and nucleation rates (Table 3) shows that the nucleation kinetics are similar. It can therefore be concluded that the three-phase line does not have a dominant influence on nucleation kinetics for THF hydrates, unlike CO_2 hydrates.[29] This is a rational conclusion since CO_2 and water are physically separated at the 3-phase line (which is therefore expected to be the nucleation site), whereas water and THF are completely mixed in the present experiments and do not critically need a surface to nucleate.

Table 3. Summary of the Nucleation Rates for Various Experiments in This Study

Exp. ID	Test type	Nucleation rate (min^{-1})
1	DI water without Mg promotion	0.00107
2	DI water with Mg promotion	0.0132
3	DI water with Mg and accelerated cooling	0.0567
5	DI water with Mg and 3-phase line	0.0156
6	Salt water without Mg promotion	1.49×10^{-4}
7	Salt water with Mg promoter	0.0148

Another experimental run was conducted to study the influence of magnesium on the memory effect.[11,12] These experiments were conducted by forming THF hydrates using a magnesium plate, dissociating the hydrates, and then reforming the hydrates from the same solution again. The expectation was that if the memory effect has a role, then the induction time will be shorter for dissociated-hydrate water. To comprehensively test this phenomenon, experiments were conducted where THF hydrates were dissociated at three different temperatures (5 , 10, 22 °C). Subsequent formation experiments were conducted immediately afterward. For the 10 and 22 °C dissociation temperatures, we measured no meaningful difference in the induction times between fresh water and dissociated-hydrate water; the average induction times for these cases were 56 and 64 min, respectively, which is similar to other data in Table 2. However, for the 5 °C dissociation temperature, we observed a 2.7X reduction in induction time during reformation, which is significant (more details contained in Table S2). These experiments show that the memory effect does exist with THF hydrates, but that it is strongly dependent on specific conditions associated with THF hydrate formation. We also note that a detailed study of the memory effect was beyond the scope of this study.

Calculation of Nucleation Rate. Previous sections quantified the nucleation promotion benefits of magnesium by focusing on the induction time. A better metric for comparison of various promoters is the nucleation rate. Based on procedures developed in a previous study,[35] the nucleation rate, J, can be calculated by fitting $P(t) = 1 - \exp(-Jt)$ to the induction time data recorded in the current study. $P(t)$ is the probability that hydrates will nucleate at a given subcooling and at a given time t. The obtained nucleation rate for each of our studies is presented in Table 3 (additional details are presented in Figure S2). Based on the nucleation rates, the most favorable formation is the case with the strongest driving force—deionized water and THF solution with the cooling bath set to −5 °C (accelerated cooling). The results in Table 3 show that magnesium-based promotion increases the nucleation rates by a factor of 12 for deionized water and by a factor of 99 for saltwater; these are very significant enhancements.

Experiments to Study Nucleation Promotion via Magnesium Ions. This study clearly highlights the nucleation-promoting influence of magnesium. Additional experiments were conducted with the objective of obtaining insights into the mechanisms underlying nucleation promotion. One particular objective of these experiments was to determine whether magnesium ions in solution are responsible for promotion. A previous study[36] from the present group uncovered evidence of aluminum-ion-complex-based coordination compounds promoting the electronucleation of THF. Also, magnesium reacts slowly with water, which should result in magnesium ions in solution (from $Mg(OH)_2$ formation). Accordingly, experiments were conducted to determine whether water previously exposed to magnesium can subsequently nucleate THF hydrates. For these experiments,

https://doi.org/10.1021/acs.langmuir.4c02882
Langmuir XXXX, XXX, XXX−XXX

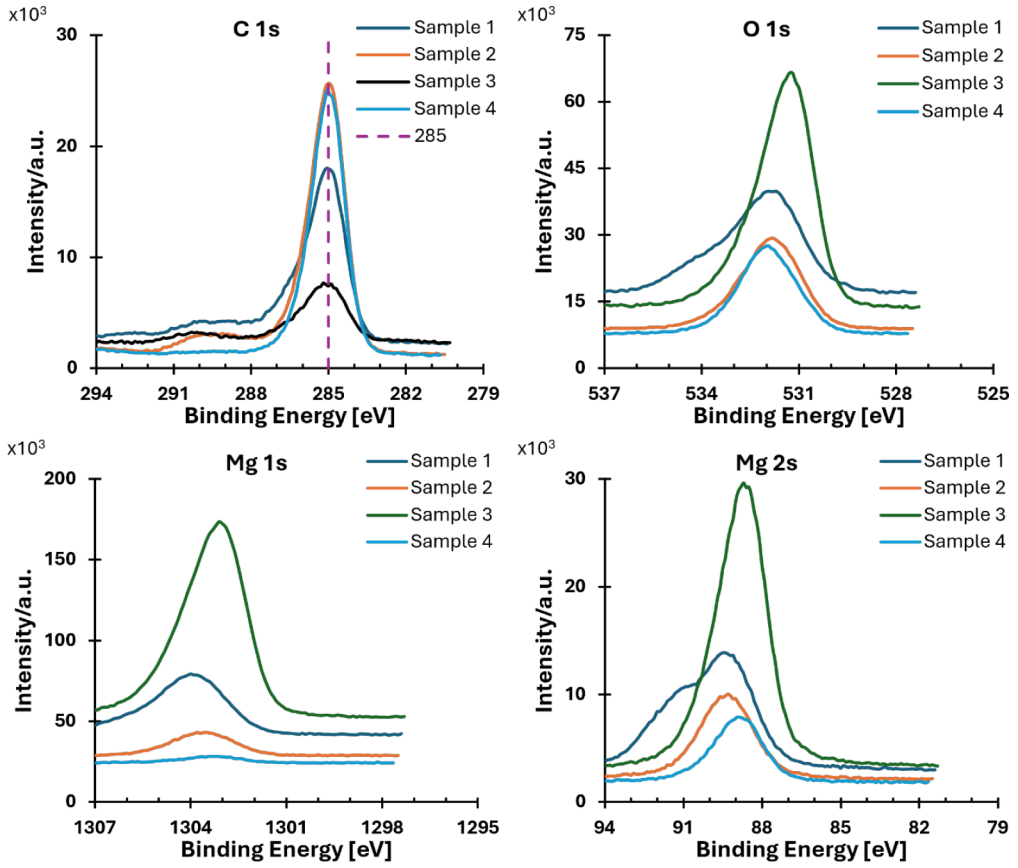

Figure 6. XPS analysis of magnesium plates in the O 1s, C 1s, O 1s, and O 2s regions.

magnesium plates were soaked in water for 1 h, 24 h, and 1-week duration. This water was then subsequently used to make the 1:15 THF solution for the hydrate formation experiments. However, when compared to experiments without a magnesium plate in the solution, no improvement in induction time or the percentage of tubes nucleated was observed. This clearly indicates that the presence of solid magnesium in the hydrate-forming solution is essential for rapid nucleation.

Another related experiment involved dissolving two common magnesium salts in water used to form THF hydrates. These include magnesium sulfate (pure Epson salt) and magnesium carbonate (or climbing chalk). Magnesium sulfate at two different concentrations (2.5 and 5 wt %) was dissolved in water used for THF hydrate formation. The 5 wt % concentration showed reduced induction time; the average induction time was 240 min compared to 367 min with no promoters (i.e., a 1.6× reduction) with 100% of tubes nucleating. However, the 2.5 wt % concentration was observed to have no impact on reducing induction time, and only 53% of tubes nucleated. Given the results with $MgSO_4$ promoter, only a 5 wt % concentration study was conducted for $MgCO_3$. However, no improvement in induction time nor percentage of tubes nucleating was observed in the presence of magnesium carbonate (full induction time details can be found in Table S1). These studies suggest that the influence of magnesium ions on nucleation is not very strong and manifests above a threshold concentration. The relative solubilities of $MgSO_4$, $MgCO_3$, and $Mg(OH)_2$ ($MgSO_4 \gg MgCO_3 \gg Mg(OH)_2$) in water determine the amount of magnesium ions available to promote nucleation.

The above two groups of experiments (water previously exposed to magnesium and water with magnesium salts) clearly suggest that the presence of solid magnesium in solution is critical to nucleation promotion. While previously dissolved magnesium ions do play a role in influencing nucleation, it appears to be a secondary effect. This finding is in sync with another study[35] from the present group, wherein dissolved aluminum salts failed to replicate the nucleation promotion behavior of pure aluminum surfaces for CO_2 hydrate nucleation. The active reaction of water with magnesium and possible nanobubble generation on the magnesium surface are likely significantly responsible for nucleation promotion (discussed ahead).

Post-experiments Characterization of Magnesium Surfaces. To obtain more detailed insights into the interfacial mechanisms occurring during Mg-promoted hydrate formation, XPS analysis was conducted on magnesium plates after experiments. In particular, the analysis was conducted on four samples. Sample 1 corresponds to the magnesium plate used in the near-instantaneous nucleation experiment in DI water (exp. ID 4). Sample 2 is the magnesium plate associated with hydrate formation in DI water (exp. ID 2). Sample 3 corresponds to hydrate formation in saltwater (exp. ID 7), and sample 4 is an unused Mg sample (control).

XPS analysis (Figure 6) shows the effect of different experimental conditions on the nucleation of tetrahydrofuran (THF) hydrates (wide spectra analysis is in Figure S3). Sample 1's detailed O 1s region clearly shows two main peaks: one close to 532 eV associated with oxygen bonded to carbon and, most probably, also at lower binding energy (~531 eV), to oxygen from $Mg(OH)_2$ or MgO;[37,38] and another one at ~534

https://doi.org/10.1021/acs.langmuir.4c02882
Langmuir XXXX, XXX, XXX−XXX

eV revealing the presence of structured bonded water. This suggests that the intermolecular forces present were mainly strong hydrogen bridge type, which can facilitate the formation of hydrates. Sample 2 reveals a larger relative amount of aliphatic carbon than sample 1, which attenuates the XPS photoelectron signal of magnesium (Mg 1s and Mg 2s). Sample 3 also shows water, as attested by the asymmetry of the O 1s peak at the high-binding-energy side, and an overall large amount of oxygen, which is likely due to the presence of MgO, formed by the oxidation of Mg in the presence of an ionic solution (NaCl, 3.5 wt %). Nevertheless, it is interesting to notice that in samples 1 and 3, C 1s regions show a small shoulder centered at ∼287 eV (more intense in sample 1), which is hardly perceptible in sample 2 and absent in sample 4, assigned to carbon singly bonded to oxygen,[37] compatible with the presence of C−O−C from THF.

Mg 1s and Mg 2s spectra show that sample 4's magnesium plate is covered by a carbonaceous layer, confirmed by the C 1s peak attributed to a relatively large amount of aliphatic carbon (from cleaning solvents). This carbon overlayer attenuates the photoelectron signals from Mg 1s and Mg 2s. Another interesting feature is the difference in the Mg 2s spectra for samples 1 and 3. They are the ones with higher Mg reactivity at the surface; however, the XPS peaks are not identical. This can be an indication that the fluorine present in sample 1 may be playing a role in the nucleation rates. In the case of sample 2 where there is only DI water (a molecular solvent) present, data show a lower nucleation rate than sample 3, which utilizes an ionic solvent.

The difference in the Mg 1s and Mg 2s spectra also points to reactivity at the surface of magnesium with different rates of exposure. Considering that the media used in this study (DI water and salt water) are very different from each other, these results suggest that two different formation mechanisms are likely responsible, with Mg playing an important role in both. Mg 1s photoelectrons have much lower KE than Mg 2s photoelectrons, which means that in the Mg 1s spectra, photoelectrons come from an outer layer than the ones detected in Mg 2s. The differences observed, particularly in Mg 2s, show that sample 1's surface has some stratification, meaning that at the surface, Mg is found in different chemical vicinities, the shoulder centered at ∼91 eV being assigned to Mg in a very electronegative neighborhood or, alternatively, Mg in a less conductive layer than the Mg detected at ∼89 eV. Besides Mg, other ions may accelerate nucleation by acting as nucleation sites for the kinetic promotion effect. In these studies, this effect is observed in the differences between samples 1−3 and sample 4. Overall, XPS analysis indicates a strong role of Mg in promoting the THF hydrate nucleation. This also highlights the need for detailed in situ characterization to nail down the specific promoting mechanism. Importantly, the analysis did not show any evidence of other components of the magnesium alloy (96% magnesium, 3% aluminum, and 1% zinc) playing a role in nucleation promotion.

While XPS analysis outlines chemical pathways to nucleation promotion, mechanistic effects related to the reaction between water and magnesium are also likely at play. The hypothesis outlined in a previous study[29] is that very small amounts of hydrogen are produced on the surface in the form of nanobubbles that can act as nucleation sites. The present group has previously shown that surface bubbles can enhance nucleation;[39] nanobubbles produced on the surface of magnesium could aid any chemical promotion pathways.

Our hypotheses are supported by recent research. A recent study by Li et al.[40] confirms our group's previous finding[29] that magnesium strongly promotes CO_2 hydrate nucleation (which motivated the present study). This study[40] analyzes the reactions between magnesium and the solution to suggest possible reasons for promotion: corrosion due to the acidic environment and reaction with water can produce hydrogen bubbles which act as nucleation sites. Additionally, the dissolution of magnesium ions into solution can also play a role. Feng et al.[41] have recently published a study regarding the impact nanobubbles have on the promotion of hydrate nucleation. Various gases were bubbled into a reactor where methane hydrates were being formed; nucleation promotion was seen regardless of the gas being bubbled. We also have our own detailed study published very recently,[42] which showed that CO_2 hydrates form very quickly and more densely in a bubble column reactor compared to a static case. Overall, it is very likely that a combination of bubble-related and chemistry-related aspects jointly promotes nucleation

Outlook for Magnesium-Promoted Nucleation. It should be noted that very little magnesium is consumed in these experiments. Weight measurements pre- and post-experiment were conducted for experiments with both DI and saltwater. For experiments with DI water, no measurable weight difference in the magnesium plate was detected. Magnesium did corrode and lose mass in saltwater experiments but at a very slow rate of 1.49×10^{-5} g/mm^2; however, this should not be treated as a measure of consumption of magnesium. Importantly, magnesium was in contact with water for many hours in these experiments, although its useful role was limited to the first few minutes only. This again suggests that very small quantities of magnesium are consumed during hydrate formation and that magnesium essentially acts like a catalyst.

Magnesium usage is in sharp contrast to the relatively large quantities of traditional chemical promoters used to form hydrates. As an illustration, 500 ppm concentration of SDS is typically used for hydrate formation promotion.[43] The cost per gram of Mg alloy plate used in this study is $3.60, while the cost per gram of SDS is $0.60. Although the price per gram for Mg is higher, the consumption of Mg is negligible, while the entire amount of SDS will be consumed. Considering the negligible consumption of Mg, the cost for using Mg is much lower than that of traditional promoters. Furthermore, there are significant costs associated with chemical handling due to environmental issues. All these aspects highlight the importance of magnesium for hydrate promotion from a techno-economic and environmental perspective. However, it should be noted that SDS assists both the nucleation and growth of hydrates, while the role of magnesium is primarily to catalyze nucleation.

CONCLUSIONS

Magnesium shows significant catalytic ability to accelerate nucleation of THF hydrates without the use of any other promoters or mechanical or electrical stimuli. Importantly, we show that near-instantaneous nucleation is possible, which opens the door for applications that require "nucleation-on-demand". Through detailed and systematic experiments, we uncover the role of various parameters (contact line and cooling rate) in nucleation promotion. Post-experiments XPS

https://doi.org/10.1021/acs.langmuir.4c02882
Langmuir XXXX, XXX, XXX−XXX

analysis provides several insights into the mechanisms (chemical and mechanistic) underlying hydrate nucleation promotion.

■ ASSOCIATED CONTENT

Supporting Information

The Supporting Information is available free of charge at https://pubs.acs.org/doi/10.1021/acs.langmuir.4c02882.

Experimental setup, experiments on memory effect, experiments involving magnesium ions, nucleation rate calculations, and XPS analysis (PDF)

Nucleation and growth of THF hydrates (MP4)

Near-instantaneous nucleation of THF hydrates (MP4)

■ AUTHOR INFORMATION

Corresponding Author

Vaibhav Bahadur − *Walker Department of Mechanical Engineering, The University of Texas at Austin, Austin, Texas 78712, United States;* orcid.org/0000-0001-7442-7769; Email: vb@austin.utexas.edu

Authors

Karey Maynor − *Walker Department of Mechanical Engineering, The University of Texas at Austin, Austin, Texas 78712, United States;* orcid.org/0009-0009-3351-8408

Awan Bhati − *Walker Department of Mechanical Engineering, The University of Texas at Austin, Austin, Texas 78712, United States*

Mark Hamalian − *Walker Department of Mechanical Engineering, The University of Texas at Austin, Austin, Texas 78712, United States*

Ana Maria Ferraria − *Institute for Bioengineering and Biosciences and Departamento de Engenharia Química, Instituto Superior Técnico, and Associate Laboratory i4HB−Institute for Health and Bioeconomy at Instituto Superior Técnico, Universidade de Lisboa, Lisbon 1049-001, Portugal;* orcid.org/0000-0002-6784-6540

Ana Paula da Costa Ribeiro − *Centro de Química Estrutural, Institute of Molecular Sciences, Departamento de Engenharia Química, Instituto Superior Técnico, Universidade de Lisboa, Lisboa 1049-001, Portugal*

Ana S. Moita − *IN+, Center for Innovation, Technology and Policy Research, Instituto Superior Técnico, University of Lisbon, Lisboa 1049-001, Portugal*

Complete contact information is available at: https://pubs.acs.org/10.1021/acs.langmuir.4c02882

Author Contributions

K.M.: conceptualization, methodology, investigation, data analysis, writing, editing. A.B.: investigation and editing. M.H.: investigation. A.M.F.: investigation, analysis. A.P.da.C.R.: investigation, analysis, writing. A.S.M.: analysis. V.B.: conceptualization, methodology, investigation, writing, editing.

Notes

The authors declare no competing financial interest.

■ ACKNOWLEDGMENTS

This study was supported by NSF grants 2234604, 1653412, and 2202071, along with support from the Energy Institute at UT Austin. The authors also acknowledge Fundação para a Ciência e a Tecnologia−FCT for partially supporting this research through project 2022.15778.UTA (UT Austin Portugal Program). Karey Maynor and Mark Hamalian acknowledge NSF Graduate Fellowships. The authors also acknowledge the assistance of Hugo Celio at UT Austin for conducting XPS studies. The acquisition of the VersaProbe-IV XPS was supported by the National Science Foundation Major Research Instrumentation program (Grant No. 2117623).

■ REFERENCES

(1) Sloan, J. E. D.; Koh, C. A. *Clathrate Hydrates of Natural Gases*, 3 rd ed.; CRC Press, Taylor Francis Group: New York, 2008.

(2) Ismail, N. A.; Koh, C. A. Growth Rate and Morphology Study of Tetrahydrofuran Hydrate Single Crystals and the Effect of Salt. *CrystEngcomm* **2022**, *24* (23), 4301−4311.

(3) Linga, P.; Adeyemo, A.; Englezos, P. Medium-Pressure Clathrate Hydrate/Membrane Hybrid Process for Postcombustion Capture of Carbon Dioxide. *Environ. Sci. Technol.* **2008**, *42* (1), 315−320.

(4) Wang, F.; Mu, J.; Lin, W.; Cao, Y.; Wang, Y.; Leng, S.; Guo, L.; Zhou, Y. Post-Combustion CO2 Capture via the Hydrate Formation at the Gas-Liquid-Solid Interface Induced by the Non-Surfactant Graphene Oxide. *Energy* **2024**, *290*, 130177.

(5) Phan, A.; Schlösser, H.; Striolo, A. Molecular Mechanisms by Which Tetrahydrofuran Affects CO2 Hydrate Growth: Implications for Carbon Storage. *Chem. Eng. J.* **2021**, *418*, 129423.

(6) Kang, K. C.; Linga, P.; Park, K.; Choi, S.-J.; Lee, J. D. Seawater Desalination by Gas Hydrate Process and Removal Characteristics of Dissolved Ions (Na+, K+, Mg2+, Ca2+, B3+, Cl−, SO42−). *Desalination* **2014**, *353*, 84−90.

(7) Lee, Y.; Seo, D.; Lee, S.; Park, Y. Advances in Nanomaterials for Sustainable Gas Separation and Storage: Focus on Clathrate Hydrates. *Acc. Chem. Res.* **2023**, *56* (22), 3111−3120.

(8) Kang, D. W.; Lee, W.; Ahn, Y.-H.; Kim, K.; Lee, J. W. Facile and Sustainable Methane Storage via Clathrate Hydrate Formation with Low Dosage Promoters in a Sponge Matrix. *Energy* **2024**, *292*, 130631.

(9) Ogata, K.; Hashimoto, S.; Sugahara, T.; Moritoki, M.; Sato, H.; Ohgaki, K. Storage Capacity of Hydrogen in Tetrahydrofuran Hydrate. *Chem. Eng. Sci.* **2008**, *63* (23), 5714−5718.

(10) Conrad, H.; Lehmkühler, F.; Sternemann, C.; Sakko, A.; Paschek, D.; Simonelli, L.; Huotari, S.; Feroughi, O.; Tolan, M.; Hämäläinen, K. Tetrahydrofuran Clathrate Hydrate Formation. *Phys. Rev. Lett.* **2009**, *103* (21), 218301.

(11) Wilson, P. W.; Haymet, A. D. J. Hydrate Formation and Re-Formation in Nucleating THF/Water Mixtures Show No Evidence to Support a "Memory" Effect. *Chem. Eng. J.* **2010**, *161* (1−2), 146−150.

(12) Liu, W.; Wang, S.; Yang, M.; Song, Y.; Wang, S.; Zhao, J. Investigation of the Induction Time for THF Hydrate Formation in Porous Media. *J. Nat. Gas Sci. Eng.* **2015**, *24*, 357−364.

(13) Gough, S. R.; Davidson, D. W. Composition of Tetrahydrofuran Hydrate and the Effect of Pressure on the Decomposition. *Can. J. Chem.* **1971**, *49* (16), 2691−2699.

(14) Makogan, T. Y.; Larsen, R.; Knight, C. A.; Sloan, J. E. D. Melt Growth of Tetrahydrofuran Clathrate Hydrate and Its Inhibition: Method and First Results. *J. Cryst. Growth* **1997**, *179* (179), 258−262.

(15) Lewis, R. *Chemistry*, 3 rd ed.; Palgrave Macmillan Ltd.: Basingstoke, 2006.

(16) Vlasic, T. M.; Servio, P. D.; Rey, A. D. THF Hydrates as Model Systems for Natural Gas Hydrates: Comparing Their Mechanical and Vibrational Properties. *Ind. Eng. Chem. Res.* **2019**, *58* (36), 16588−16596.

(17) Kida, M.; Yoneda, J.; Masui, A.; Konno, Y.; Jin, Y.; Nagao, J. Mechanical Properties of Polycrystalline Tetrahydrofuran Hydrates as Analogs for Massive Natural Gas Hydrates. *J. Nat. Gas Sci. Eng.* **2021**, *96*, 104284.

(18) Hoseinynezhad, E.; Varaminian, F. The Effect of Sodium Halide Salts on the Kinetics of Tetrahydrofuran Hydrate Formation by Using a Differential Scanning Calorimetry Method. *J. Mol. Liq.* **2019**, *292*, 111279.

(19) Dai, S.; Lee, J. Y.; Santamarina, J. C. Hydrate Nucleation in Quiescent and Dynamic Conditions. *Fluid Phase Equilib.* **2014**, *378*, 107−112.
(20) Carpenter, K.; Bahadur, V. Electronucleation for Rapid and Controlled Formation of Hydrates. *J. Phys. Chem. Lett.* **2016**, *7* (13), 2465−2469.
(21) Chen, B.; Dong, H.; Sun, H.; Wang, P.; Yang, L. Effect of a Weak Electric Field on THF Hydrate Formation: Induction Time and Morphology. *J. Pet. Sci. Eng.* **2020**, *194*, 107486.
(22) Devarakonda, S.; Groysman, A.; Myerson, A. S. THF−Water Hydrate Crystallization: An Experimental Investigation. *J. Cryst. Growth* **1999**, *204* (4), 525−538.
(23) Yang, M.; Liu, W.; Song, Y.; Ruan, X.; Wang, X.; Zhao, J.; Jiang, L.; Li, Q. Effects of Additive Mixture (THF/SDS) on the Thermodynamic and Kinetic Properties of CO_2 /H_2 Hydrate in Porous Media. *Ind. Eng. Chem. Res.* **2013**, *52* (13), 4911−4918.
(24) Zhang, J.; Li, Y.; Yin, Z.; Zheng, X. Y.; Linga, P. How THF Tunes the Kinetics of H_2 − THF Hydrates? A Kinetic Study with Morphology and Calorimetric Analysis. *Ind. Eng. Chem. Res.* **2023**, *62* (51), 21918−21932.
(25) Sabil, K. M.; Román, V. R.; Witkamp, G.-J.; Peters, C. J. Experimental Observations on the Competing Effect of Tetrahydrofuran and an Electrolyte and the Strength of Hydrate Inhibition among Metal Halides in Mixed CO2 Hydrate Equilibria. *J. Chem. Thermodyn.* **2010**, *42* (3), 400−408.
(26) Sun, S.; Peng, X.; Zhang, Y.; Zhao, J.; Kong, Y. Stochastic Nature of Nucleation and Growth Kinetics of THF Hydrate. *J. Chem. Thermodyn.* **2017**, *107*, 141−152.
(27) Sun, C.; Liu, S.; Li, S.; Wang, K.; Sun, Y.; Li, X.; Zhang, Z. Role of Nano-SiO_2 Dispersion in Tetrahydrofuran Hydrate Induction Time through Image Analyses. *Energy Fuels* **2023**, *37* (17), 13181−13190.
(28) Nashed, O.; Partoon, B.; Lal, B.; Sabil, K. M.; Shariff, A. M. Review the Impact of Nanoparticles on the Thermodynamics and Kinetics of Gas Hydrate Formation. *J. Nat. Gas Sci. Eng.* **2018**, *55*, 452−465.
(29) Kar, A.; Acharya, P. V.; Bhati, A.; Mhadeshwar, A.; Venkataraman, P.; Barckholtz, T. A.; Celio, H.; Mangolini, F.; Bahadur, V. Magnesium-Promoted Rapid Nucleation of Carbon Dioxide Hydrates. *ACS Sustainable Chem. Eng.* **2021**, *9* (33), 11137−11146.
(30) Kar, A.; Bhati, A.; Lokanathan, M.; Bahadur, V. Faster Nucleation of Ice at the Three-Phase Contact Line: Influence of Interfacial Chemistry. *Langmuir* **2021**, *37* (43), 12673−12680.
(31) Veluswamy, H. P.; Linga, P. Natural Gas Hydrate Formation Using Saline/Seawater for Gas Storage Application. *Energy Fuels* **2021**, *35* (7), 5988−6002.
(32) Holzammer, C.; Finckenstein, A.; Will, S.; Braeuer, A. S. How Sodium Chloride Salt Inhibits the Formation of CO_2 Gas Hydrates. *J. Phys. Chem. B* **2016**, *120* (9), 2452−2459.
(33) Mohammadi, A. H.; Kraouti, I.; Richon, D. Methane Hydrate Phase Equilibrium in the Presence of NaBr, KBr, CaBr2, K2CO3, and MgCl2 Aqueous Solutions: Experimental Measurements and Predictions of Dissociation Conditions. *J. Chem. Thermodyn.* **2009**, *41* (6), 779−782.
(34) Kharrat, M.; Dalmazzone, D. Experimental Determination of Stability Conditions of Methane Hydrate in Aqueous Calcium Chloride Solutions Using High Pressure Differential Scanning Calorimetry. *J. Chem. Thermodyn.* **2003**, *35* (9), 1489−1505.
(35) Acharya, P. V.; Kar, A.; Shahriari, A.; Bhati, A.; Mhadeshwar, A.; Bahadur, V. Aluminum-Based Promotion of Nucleation of Carbon Dioxide Hydrates. *J. Phys. Chem. Lett.* **2020**, *11* (4), 1477−1482.
(36) Shahriari, A.; Acharya, P. V.; Carpenter, K.; Bahadur, V. Metal-Foam-Based Ultrafast Electronucleation of Hydrates at Low Voltages. *Langmuir* **2017**, *33* (23), 5652−5656.
(37) Beamson, G.; Briggs, D. High Resolution XPS of Organic Polymers: The Scienta ESCA300 Database. *J. Chem. Educ.* **1993**, *70* (1), A25.
(38) National Institute of Standards and Technology. *X-Ray Photoelectron Spectroscopy Database*. NIST2012.
(39) Carpenter, K.; Bahadur, V. Electrofreezing of Water Droplets under Electrowetting Fields. *Langmuir* **2015**, *31* (7), 2243−2248.
(40) Li, Y.; Yin, Z.; Rao, Y.; Lu, H.; Xu, C.; Liu, X.; Li, Y.; Zhao, J.; Linga, P. Ultrarapid CO_2 Hydrate Nucleation and Growth Enabled by Magnesium Coupled with Amino Acids as a Promoter. *Energy Fuels* **2024**, *38* (17), 16543−16554.
(41) Feng, Y.; Han, Y.; Gao, P.; Kuang, Y.; Yang, L.; Zhao, J.; Song, Y. Study of Hydrate Nucleation and Growth Aided by Micro-Nanobubbles: Probing the Hydrate Memory Effect. *Energy* **2024**, *290*, 130228.
(42) Bhati, A.; Hamalian, M.; Acharya, P. V.; Bahadur, V. Ultrafast Formation of Carbon Dioxide Hydrate Foam for Carbon Sequestration. *ACS Sustainable Chem. Eng.* **2024**, *12* (29), 11013−11023.
(43) Nasir, Q.; Suleman, H.; Elsheikh, Y. A. A Review on the Role and Impact of Various Additives as Promoters/ Inhibitors for Gas Hydrate Formation. *J. Nat. Gas Sci. Eng.* **2020**, *76*, 103211.

https://doi.org/10.1021/acs.langmuir.4c02882
Langmuir XXXX, XXX, XXX−XXX